Observation of bimolecular recombination in high mobility semiconductor Bi_2O_2Se using ultrafast spectroscopy

Chunhui Zhu, Tong Tong, Yujie Liu, Yafei Meng, Zhonghui Nie, Xuefeng Wang, Yongbing Xu, Yi Shi, Rong Zhang, and Fengqiu Wang

Citation: Appl. Phys. Lett. **113**, 061104 (2018); doi: 10.1063/1.5037026
View online: https://doi.org/10.1063/1.5037026
View Table of Contents: http://aip.scitation.org/toc/apl/113/6
Published by the American Institute of Physics

Observation of bimolecular recombination in high mobility semiconductor Bi_2O_2Se using ultrafast spectroscopy

Chunhui Zhu,[a] Tong Tong,[a] Yujie Liu, Yafei Meng, Zhonghui Nie, Xuefeng Wang,[b] Yongbing Xu, Yi Shi, Rong Zhang, and Fengqiu Wang[b]
School of Electronic Science and Engineering and Collaborative Innovation Center of Advanced Microstructures, Nanjing University, Nanjing 210093, China

(Received 20 April 2018; accepted 23 July 2018; published online 7 August 2018)

Bi_2O_2Se is emerging as a high mobility functional material for optoelectronics, but its fundamental optical properties remain less well studied. Here, ultrafast photocarrier dynamics in single crystal Bi_2O_2Se is investigated by pump fluence-dependent, broadband ultrafast spectroscopy. Our results reveal that bimolecular recombination plays an important role in the photocarrier relaxation process, and a room-temperature bimolecular recombination constant of $(1.29 \pm 0.42) \times 10^{-9}\,cm^{-3}\ s^{-1}$ is obtained for Bi_2O_2Se. Such a level of the recombination constant combined with a high mobility ($\sim$1006 $cm^2\ V^{-1}\ s^{-1}$ at 200 K for Bi_2O_2Se) suggests that Bi_2O_2Se can be a promising material for photovoltaic applications. *Published by AIP Publishing.* https://doi.org/10.1063/1.5037026

High mobility two-dimensional (2D) materials have received significant attention in the past decade, since they offer huge potential for the next-generation photonics and electronic technologies.[1–6] Graphene is a capable representative material for emerging 2D materials, not only because it is the first to be isolated and studied but also because of a range of fascinating physical properties due to its unique electronic structure, such as high carrier mobility, typically 10 000–70 000 $cm^2\ V^{-1}\ s^{-2}$ on the SiO_2/Si substrate.[7,8] It is well known that the absence of a bandgap in graphene renders the on/off ratio of graphene field-effect transistors (FETs) orders of magnitude lower than that of silicon-based FET, posing a significant challenge for its application in digital electronics.[8] To date, in addition to graphene, a number of 2D materials (e.g., layered transition-metal dichalcogenides and black phosphorus) have been uncovered. Black phosphorus may offer a desirable on/off ratio but exhibit compromised environmental stability. The quest for materials with a high mobility level as required for high performance FET devices is still on.[4]

Bi_2O_2Se, a layered indirect bandgap semiconductor material, has recently attracted renewed interest due to its tunable bandgap (1.37–1.9 eV when reduced from bulk to monolayer) as well as the demonstration of very high Hall mobility (20 000 $cm^2\ V^{-1}\ s^{-2}$) in its ultrathin form.[9] As a conventional thermoelectric material, Bi_2O_2Se has been extensively investigated as a candidate for achieving high thermoelectric conversion efficiency,[10] and now, a variety of optoelectronic applications, including high-speed FETs and photodetectors, have been proposed and demonstrated based on this novel material.[9,11,12] By contrast, the investigation of the optical properties, i.e., photocarrier dynamics, of this potentially important material has been scarce and the physical mechanisms underpinning the relaxation behaviors are unclear. In particular, transport behaviors in a high-speed device are known to be closely related to the relaxation dynamics of hot carriers, which are generated by the presence of high fields and/or dynamic fields in the material.[13] Understanding the ultrafast carrier dynamics is, therefore, of critical importance to the design and optimizations of high-speed devices.

Ultrafast spectroscopy is a powerful technique that has been used to reveal the photocarrier relaxation dynamics in both 2D materials and other quantum materials.[14–18] In this work, using pump fluence-dependent ultrafast spectroscopy, we demonstrate that the initial photocarrier relaxation in single crystal Bi_2O_2Se is characterized by a bimolecular recombination behavior, and the bimolecular recombination constant, γ, is determined to be $(1.29 \pm 0.42) \times 10^{-9}\,cm^{-3}\ s^{-1}$. In addition, the very small ratio of the bimolecular recombination constant to the charge carrier mobility for Bi_2O_2Se ($\sim 1.29 \times 10^{-12}$ cm V) can provide a good trade-off between the charge recombination rate and mobility, suggesting that Bi_2O_2Se is highly desirable for developing high-performance photovoltaic cells.

High quality Bi_2O_2Se single crystal samples are grown by melting stoichiometric mixtures of 99.99% purity Bi_2O_3, 99.99% purity Bi, and 99.99% purity Se elements in sealed evacuated quartz tubes. After slow cooling from the melting point down to about 730 °C over two days, crystals are kept at this temperature for several days and then cooled to room temperature.[19] The as-grown samples typically have a millimeter lateral size and exhibit a good mirror surface. Figure 1 shows the X-ray diffraction pattern of the Bi_2O_2Se sample. Only a series of (00*l*) plane diffraction peaks can be observed, confirming the good crystalline quality of our sample. Notably, this result also reveals that the mirror surface (which is used in the ultrafast spectroscopy investigation) corresponds to the *c*-axis orientation. We then conduct transport measurements on the samples by the physical property measurement system. The measured Hall resistance at 200 K is shown in Fig. 1(b). Using the linear fitted slope (−1.58 mΩ/T), sample thickness ($t \sim 172\,\mu m$), and conductivity ($\sigma \sim 3698.5$ S/cm), Hall coefficient $R_H = \frac{tV_H}{BI} = -0.272\,cm^3/C$, carrier density $n = \frac{t}{|R_H|e} = 2.3 \times 10^{19}\,cm^{-3}$, and Hall mobility

[a]C. Zhu and T. Tong contributed equally to this work.
[b]Authors to whom correspondence should be addressed: fwang@nju.edu.cn and xfwang@nju.edu.cn.

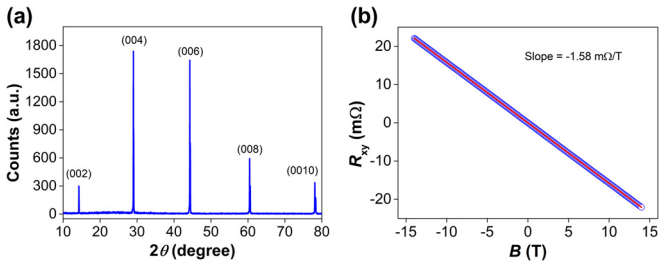

FIG. 1. (a) X-ray diffraction pattern for the Bi_2O_2Se single crystal sample. (b) Hall resistance ($R_{xy} = V_H/I$) of Bi_2O_2Se at 200 K (points) and linear fitting (solid line).

$\mu = |R_H|\sigma = 1006\,\mathrm{cm^2\,V^{-1}\,s^{-1}}$ can be obtained. The Shubnikov-de Haas (SdH) oscillations reveal an effective electron mass of $\sim 0.032 m_e$, where m_e is the free-electron mass (see supplementary Fig. S1).

For the pump-probe measurement, a 1 kHz Ti: Sapphire amplifier system (Libra, Coherent, Inc.) is used as an optical source to generate ~100 fs pulses with a central wavelength of 800 nm. The majority of the laser output energy is fed into an optical parametric amplifier to generate the probe beam with wavelengths from 800 nm to 2.5 μm, and the remaining part is used to excite photocarriers in the sample. The relative change of the reflection of the probe is recorded by a photodetector and a lock-in amplifier referenced to a 334 Hz chopped pump, to obtain differential reflection, $\Delta R/R_0 = (R - R_0)/R_0$, where R and R_0 are the reflection of the probe with and without the presence of the pump pulse, respectively. In addition, a photocarrier density of $0.8 \times 10^{19}\,\mathrm{cm^{-3}}$ for the pump fluence of 1 mJ/cm^3 is estimated by assuming that every photon excites one electron-hole pair and by using the material's absorption coefficient from the literature.[20]

Figure 2(a) shows the normalized $\Delta R/R_0$ traces at four different probe wavelengths with the pump fluence of ~1.35 mJ/cm^2. Interestingly, under our experimental conditions, the photocarrier dynamics, including signal polarity and time constants, is independent of the probe wavelength over the entire range investigated. However, the intensity of the transient reflectance is found to exhibit a monotonic dependence on the probe wavelength, i.e., stronger $\Delta R/R_0$ is obtained with increasing wavelength or decreasing photon energy, as illustrated in Fig. 2(b) (supplementary Fig. S2 shows the linear reflectance of Bi_2O_2Se that is weakly dependent on wavelengths in this infrared range). While both absorption and refractive index change can contribute to the negative transient signal, we attribute the change of the refractive

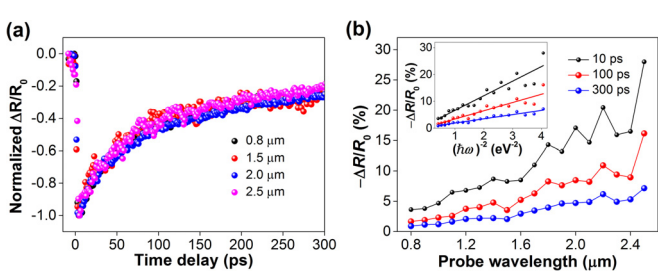

FIG. 2. Broadband pump-probe results. (a) Normalized $\Delta R/R_0$ at four different probe wavelengths. (b) Pump-probe signal intensity as a function of probe wavelength at three selected time delays, and the inset shows a linear relationship between $-\Delta R/R_0$ and $(\hbar\omega)^{-2}$.

index as the main underlying mechanism. The photocarrier induced refractive index change, originating from a Drude contribution to the dielectric function, has been demonstrated in other semiconductors, including Si, Ge, and GaAs.[21–24] In this physical picture, the fractional refractive index change can be described as

$$\frac{\Delta n}{n_0} = -\frac{2\pi e^2 N_e}{\varepsilon m^* \omega^2}, \tag{1}$$

where e, ε, m^*, ω, and N_e are the elementary charge, the dielectric constant, the reduced effective mass for electrons and holes, the angular frequency of the probing photon, and the carrier density, respectively.[24] According to the Fresnel equation, we can approximatively obtain

$$\frac{\Delta R}{R_0} \approx \frac{4\Delta n}{(n_0 - 1)^2}, \tag{2}$$

when ignoring the higher-order components.[21] In other words, under the framework of the Drude model, the transient reflectance intensity should be inversely proportional to ω^2 at a certain photoexcitation condition. In the inset of Fig. 2(b), we convert the x-axis from the wavelength to photon energy (without rescaling $-\Delta R/R_0$). The linear relationship between $-\Delta R/R_0$ and $(\hbar\omega)^{-2}$ strongly suggests that the optical response of the system can be modeled by the Drude model. To corroborate the model with our experiment, we first estimate the refractive index of the material by using its reflectance data, i.e., a $R_0 = 50\% \pm 5\%$ at 2 μm suggests an optical constant $n_0 \approx \sqrt{\varepsilon} \approx 6$ at the same wavelength. Using such a refractive index figure and combining Eqs. (1) and (2), an estimated value of $\Delta R/R_0 = -20\%$ is obtained, which is in good agreement with our experimental result of about -17%. Though believed not to be a major contribution to the signal observed in our experiment, contribution of intraband transitions should not be completely ruled out.

Before moving to discuss the physical picture of the photocarrier relaxation in Bi_2O_2Se, we present the pump fluence-dependent data obtained from a probe wavelength of 800 nm in Fig. 3(a). It can be seen that the initial stage of carrier relaxation is closely related to the pump fluences, although the $\Delta R/R_0$ peak signal scales linearly with the pump fluences [Fig. 3(b)]. By contrast, all the curves exhibit a similar dynamic behavior after 300 ps, which may be attributed to the long-lived carrier recombination since Bi_2O_2Se is an indirect bandgap semiconductor.[13,20] Pump fluence-dependent dynamical features are usually related to many-body interaction.[25] After converting the measured $\Delta R/R_0$ to the photocarrier density, a linear relationship between the reciprocal of carrier density (N^{-1}) and time delay is unambiguously observed, as shown in Fig. 3(c). This feature indicates that bimolecular recombination may play an important role in the photocarrier relaxation in Bi_2O_2Se.[26–30]

The bimolecular relaxation process can be described by a rate equation, $N_0/N = \gamma N_0 t + 1$, with the recombination constant γ.[29] To provide a quantitative assessment of bimolecular behavior, we extract γN_0 from Fig. 3(c) using a linear fitting. Similar to previous reports,[27] γN_0 is found to be proportional to carrier density as shown in Fig. 4. Then,

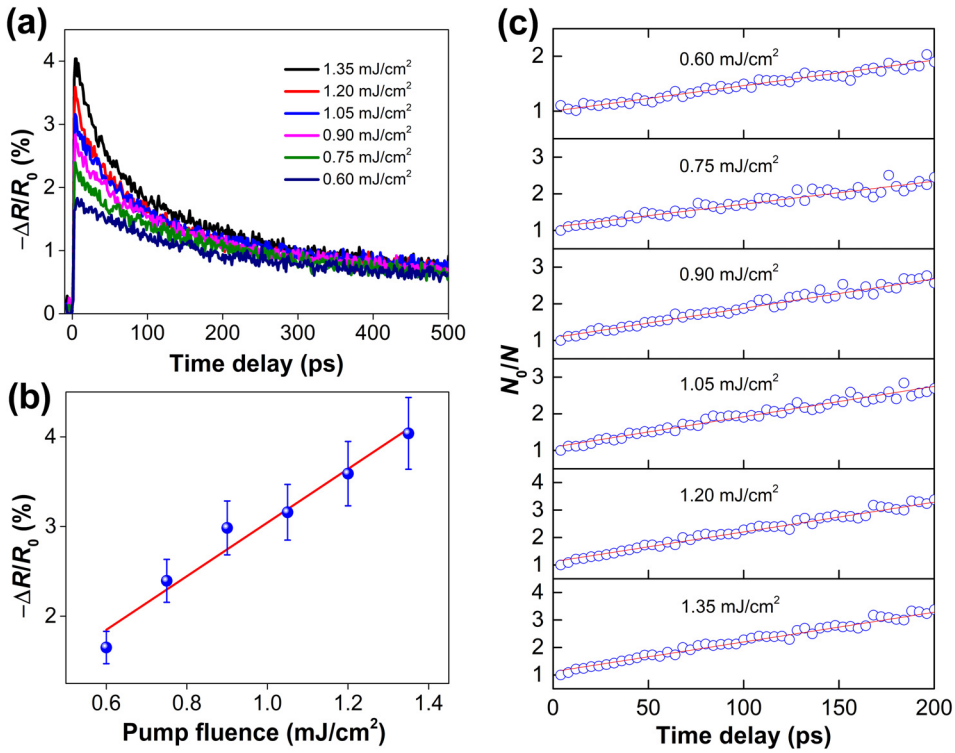

FIG. 3. Pump-fluence dependent data for the 800 nm probe. (a) Time-resolved traces. (b) Peak $\Delta R/R_0$ value. (c) The relationship between N_0/N and time delay. The solid lines in (b) and (c) correspond to linear fitting.

$\gamma = 1.06 \times 10^{-9}\,\mathrm{cm^3\ s^{-1}}$ is deduced by another linear fitting to Fig. 4. It should be noted that, as shown in the inset of Fig. 4, we have confirmed the bimolecular recombination behavior at several probe wavelengths, and a statistical value, $\gamma = (1.29 \pm 0.42) \times 10^{-9}\,\mathrm{cm^3\ s^{-1}}$, is provided by the experimental results at five different probe wavelengths, including 0.8, 1.2, 1.5 2.0, and 2.5 μm. Such a recombination rate is similar to the conventional semiconductor GaAs ($\sim 7.2 \times 10^{-10}\,\mathrm{cm^3\ s^{-1}}$) and emerging organic perovskite $CH_3NH_3PbI_3$ ($\sim 6.8 \times 10^{-10}\,\mathrm{cm^3\ s^{-1}}$).[31,32]

Using $\mu_e = 1006\,\mathrm{cm^2\ V^{-1}\ s^{-1}}$, the ratio of the bimolecular recombination constant to the charge carrier mobility, γ/μ, is estimated to be 1.29×10^{-12} cm V, which is nearly 5 orders of magnitude smaller than the value of Langevin theory, $e\varepsilon \approx 0.5 \times 10^{-7}$ cm V.[33–35] A small γ/μ allows a low charge recombination rate without the penalty of lowered charge mobility that is highly desirable for photovoltaics.[33] As noted before, several materials (e.g., amorphous silicon and organolead trihalide perovskites) whose charge recombination rates beyond the Langevin limit have been successfully incorporated in photovoltaic cells.[33–35] To gain more physical information about potential of photovoltaic applications for this material, we then evaluate the charge diffusion length (L_D) of Bi_2O_2Se by following the work of Wehrenfennig *et al.* (see supplementary Fig. S3).[36] Although the diffusion length may be underestimated by using the mono-molecular rate constant $\tau^{-1} = (500\ \mathrm{ps})^{-1}$, $L_D > 1\ \mu$m is obtained for a charge density of $<10^{18}\,\mathrm{cm^{-3}}$, approaching that of the state-of-the-art photovoltaic materials.[36,37] It should be pointed out that the bimolecular recombination rate may increase when the thickness of Bi_2O_2Se is reduced to a few-layer, because of the strong quantum confined effects in a two-dimensional system.[27] It has been demonstrated that 6 nm Bi_2O_2Se ultrathin films exhibit similar physical properties to their bulk form. Therefore, for practical solar cells where the typical thickness of absorber layers is >100 nm,[37] our results are directly relevant.

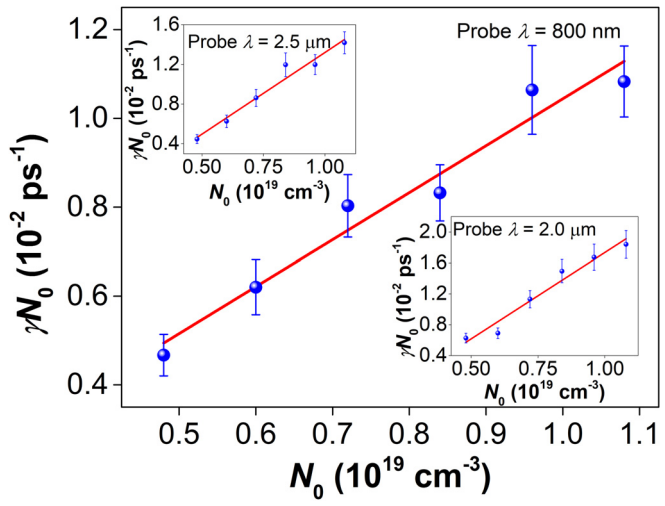

FIG. 4. The fitted γN_0 from Fig. 3(c), and the solid line is a linear fitting to obtain γ. The inset shows two similar results at the other wavelengths.

In conclusion, the single crystal Bi_2O_2Se sample is investigated by pump fluence-dependent ultrafast spectroscopy investigation. The optical response is found primarily due to the change in the refractive index. While the time constants for Bi_2O_2Se are largely independent of probe wavelength, an interesting and strong bimolecular recombination signature is observed. The bimolecular recombination constant is found to be $(1.29 \pm 0.42) \times 10^{-9}\,\mathrm{cm^{-3}\ s^{-1}}$, and the ratio of the bimolecular recombination constant to the charge carrier mobility is about 1.29×10^{-12} cm V. Such a small ratio can provide a good trade-off between the charge recombination rate and mobility. Our results shed light on the photocarrier dynamics of Bi_2O_2Se and reveal its potential use for optoelectronic devices, e.g., solar cells.

See supplementary material for the Shubnikov-de Haas (SdH) oscillations of Bi_2O_2Se, the linear reflectance of Bi_2O_2Se, and the calculated diffusion length of Bi_2O_2Se.

This work was supported in part by the State Key Project of Research and Development of China (No. 2017YFA0206304), the National Basic Research Program of China (Nos. 2014CB921101 and 2011CB301900), the National Natural Science Foundation of China (Nos. 61775093, 61378025, 61427812, U1732159, and 11774160), the National Young 1000 Talent Plan, A "Jiangsu Shuangchuang Team" Program, and Jiangsu NSF (Nos. BK20170012 and BK20140054).

[1]A. K. Geim and K. S. Novoselov, Nat. Mater. **6**, 183–191 (2007).
[2]Q. H. Wang, K. Kalantar-Zadeh, A. Kis, J. N. Coleman, and M. S. Strano, Nat. Nanotechnol. **7**, 699–712 (2012).
[3]F. Xia, H. Wang, D. Xiao, M. Dubey, and A. Ramasubramaniam, Nat. Photonics **8**, 899–907 (2014).
[4]G. Fiori, F. Bonaccorso, G. Iannaccone, T. Palacios, D. Neumaier, A. Seabaugh, S. K. Banerjee, and L. Colombo, Nat. Nanotechnol. **9**, 768–779 (2014).
[5]D. Akinwande, N. Petrone, and J. Hone, Nat. Commun. **5**, 5678 (2014).
[6]Z. Sun, A. Martinez, and F. Wang, Nat. Photonics **10**, 227–238 (2016).
[7]S. D. Sarma, S. Adam, E. H. Hwang, and E. Rossi, Rev. Mod. Phys. **83**, 407–470 (2011).
[8]F. Schwierz, Nat. Nanotechnol. **5**, 487–496 (2010).
[9]J. Wu, H. Yuan, M. Meng, C. Chen, Y. Sun, Z. Chen, W. Dang, C. Tan, Y. Liu, J. Yin, Y. Zhou, S. Huang, H. Q. Xu, Y. Cui, H. Y. Hwang, Z. Liu, Y. Chen, B. Yan, and H. Peng, Nat. Nanotechnol. **12**, 530–534 (2017).
[10]J. Yu and Q. Sun, Appl. Phys. Lett. **112**, 053901 (2018).
[11]J. Wu, Y. Liu, Z. Tan, C. Tan, J. Yin, T. Li, T. Tu, and H. Peng, Adv. Mater. **29**, 1704060 (2017).
[12]J. Li, Z. Wang, Y. Wen, J. Chu, L. Yin, R. Cheng, L. Lei, P. He, C. Jiang, L. Feng, and J. He, Adv. Funct. Mater. **28**, 1706437 (2018).
[13]J. Shah, *Hot Carriers in Semiconductor Nanostructures: Physics and Applications* (Academic Press, 1992).
[14]W. B. Cho, S. Y. Choi, C. Zhu, M. H. Kim, J. W. Kim, J. S. Kin, H. J. Park, D. H. Shin, M. Y. Jung, F. Wang, and F. Rotermund, Opt. Express **24**, 20774–20780 (2016).
[15]Z. Luo, D. Wu, B. Xu, H. Xu, Z. Cai, J. Peng, J. Weng, S. Xu, C. Zhu, F. Wang, Z. Sun, and H. Zhang, Nanoscale **8**, 1066–1072 (2016).
[16]C. Zhu, F. Wang, Y. Meng, X. Yuan, F. Xiu, H. Luo, Y. Wang, J. Li, X. Lv, L. He, Y. Xu, J. Liu, C. Zhang, Y. Shi, R. Zhang, and S. Zhu, Nat. Commun. **8**, 14111 (2017).
[17]C. Zhu, X. Yuan, F. Xiu, C. Zhang, Y. Xu, R. Zhang, Y. Shi, and F. Wang, Appl. Phys. Lett. **111**, 091101 (2017).
[18]C. Zhu, Y. Liu, J. Xu, Z. Nie, Y. Li, Y. Xu, R. Zhang, and F. Wang, Sci. Rep. **7**, 11221 (2017).
[19]T. Tong, M. Zhang, Y. Chen, Y. Li, M. Chen, J. Zhang, F. Song, X. Wang, W. Zou, Y. Xu, and R. Zhang, "Ultrahigh Hall mobility and suppressed backward scattering in layered semiconductor Bi_2O_2Se," Appl. Phys. Lett. (to be published).
[20]J. Wu, C. Tan, Z. Tan, Y. Liu, J. Yin, W. Dang, M. Wang, and H. Peng, Nano Lett. **17**, 3021–3026 (2017).
[21]M. I. Gallant and H. M. van Driel, Phys. Rev. B **26**, 2133 (1982).
[22]A. Esser, W. Kiitt, M. Strahnen, G. Maidorn, and H. Kurz, Appl. Surf. Sci. **46**, 446–450 (1990).
[23]T. Gong, P. Mertz, W. L. Nighan, and P. M. Fauchet, Appl. Phys. Lett. **59**, 721 (1991).
[24]F. E. Doany, D. Grischkowsky, and C.-C. Chi, Appl. Phys. Lett. **50**, 460–462 (1987).
[25]H. Haug and S. W. Koch, *Quantum Theory of the Optical and Electronic Properties of Semiconductors* (World Scientific, 2009).
[26]D. Sun, Y. Rao, G. A. Reider, G. Chen, Y. You, L. Brézin, A. R. Harutyunyan, and T. F. Heinz, Nano Lett. **14**, 5625–5629 (2014).
[27]N. Kumar, Q. Cui, F. Ceballos, D. He, Y. Wang, and H. Zhao, Phys. Rev. B **89**, 125427 (2014).
[28]B. Liu, Y. Meng, X. Ruan, F. Wang, W. Liu, F. Song, X. Wang, J. Wu, L. He, R. Zhang, and Y. Xu, Nanoscale **9**, 18546–18551 (2017).
[29]J. S. Manser and P. V. Kamat, Nat. Photonics **8**, 737–743 (2014).
[30]Y. Yang, M. Yang, Z. Li, R. Crisp, K. Zhu, and M. C. Beard, J. Phys. Chem. Lett. **6**, 4688–4692 (2015).
[31]Y. P. Varshni, Phys. Status Solidi B **19**, 459–514 (1967).
[32]T. W. Crothers, R. L. Milot, J. B. Patel, E. S. Parrott, J. Schlipf, P. Müller-Buschbaum, M. B. Johnston, and L. M. Herz, Nano Lett. **17**, 5782–5789 (2017).
[33]C. Wehrenfennig, G. E. Eperon, M. B. Johnston, H. J. Snaith, and L. M. Herz, Adv. Mater. **26**, 1584–1589 (2014).
[34]M. P. de Haas, J. M. Warman, and T. D. Anthopoulos, Adv. Funct. Mater. **16**, 2274 (2006).
[35]A. Pivrikas, G. Juška, A. J. Mozer, M. Scharber, K. Arlauskas, N. S. Sariciftci, H. Stubb, and R. Österbacka, Phys. Rev. Lett. **94**, 176806 (2005).
[36]C. Wehrenfennig, M. Liu, H. J. Snaith, M. B. Johnston, and L. M. Herz, Energy Environ. Sci. **7**, 2269–2275 (2014).
[37]M. Ahmadi, T. Wu, and B. Hu, Adv. Mater. **29**, 1605242 (2017).